BIOCHEMISTRY
including biophysical chemistry & molecular biology
Article

Biochemistry **2010,** *49,* 6887–6895 6887
DOI: 10.1021/bi1007386

Reversible Post-Translational Carboxylation Modulates the Enzymatic Activity of *N*-Acetyl-L-ornithine Transcarbamylase[†]

Yongdong Li,[‡,§] Xiaolin Yu,[‡] Jeremy Ho,[‡] David Fushman,[∥] Norma M. Allewell,[∥] Mendel Tuchman,[‡] and Dashuang Shi*[,‡]

[‡]*Research Center for Genetic Medicine and Department of Integrative Systems Biology, Children's National Medical Center, The George Washington University, Washington, D.C. 20010,* [§]*Key Laboratory of Organo-Pharmaceutical Chemistry, Jiangxi Province, Gannan Normal University, Ganzhou 341000, China, and* [∥]*Department of Chemistry and Biochemistry, College of Chemical and Life Sciences, University of Maryland, College Park, Maryland 20742*

Received May 10, 2010; Revised Manuscript Received July 14, 2010

ABSTRACT: *N*-Acetyl-L-ornithine transcarbamylase (AOTCase), rather than ornithine transcarbamylase (OTCase), is the essential carbamylase enzyme in the arginine biosynthesis of several plant and human pathogens. The specificity of this unique enzyme provides a potential target for controlling the spread of these pathogens. Recently, several crystal structures of AOTCase from *Xanthomonas campestris* (*xc*) have been determined. In these structures, an unexplained electron density at the tip of the Lys302 side chain was observed. Using ^{13}C NMR spectroscopy, we show herein that Lys302 is post-translationally carboxylated. The structure of wild-type AOTCase in a complex with the bisubstrate analogue N^{δ}-(phosphonoacetyl)-N^{α}-acetyl-L-ornithine (PALAO) indicates that the carboxyl group on Lys302 forms a strong hydrogen bonding network with surrounding active site residues, Lys252, Ser253, His293, and Glu92 from the adjacent subunit either directly or via a water molecule. Furthermore, the carboxyl group is involved in binding *N*-acetyl-L-ornithine via a water molecule. Activity assays with the wild-type enzyme and several mutants demonstrate that the post-translational modification of lysine 302 has an important role in catalysis.

Post-translational modification of the ε-amino group of lysine residues in proteins is a common mechanism used by organisms to regulate protein functions, including DNA−protein interactions, subcellular localization, transcriptional activity, and protein stability and activity (*1*). Lysine residues can be modified by the addition of functional groups to become acetylated, methylated, carbamylated, or carboxylated. The role of histone lysine acetylation and methylation in affecting chromatin structure and gene expression has been well-established for more than a decade (*2*). However, the biological roles for lysine carbamylation and carboxylation have rarely been investigated.

In vivo, lysine acetylation and methylation are usually conducted by acetyltransferase and methyltransferase enzymes, respectively (*3*). In addition, some proteins such as hemoglobin and human serum albumin can be acetylated nonenzymatically by chemicals such as aspirin, methyl acetyl phosphate, and other acetylating agents such as acetyl-CoA (*4*−*8*). Lysine can also be methylated by small chemicals in vitro, and this has routinely been used as a rescue method for protein crystallization (*9*). Lysine carbamylation and lysine carboxylation have been achieved only by using chemicals, and no enzyme has yet been found to catalyze these modifications. Lysine carbamylation was one of the earliest post-translational modifications of proteins to be elucidated when it was identified as a product of reversible denaturation−renaturation studies of proteins with urea (*10*, *11*). This carbamylation, which produces homocitrulline, has also been detected in uremic patients (*12*) and in patients with elevated plasma and/or urinary lysine levels (*13*). In contrast, lysine carboxylation is not as commonly reported but has been identified in a number of proteins via crystal structure determinations. In most of these proteins, the carboxyl groups of modified lysines are involved in bridging two metal ions that play a structural role in the active site. In several other proteins, however, a direct role for a carboxylated lysine in the catalytic mechanism has been reported (*14*−*16*).

N-Acetyl-L-ornithine transcarbamylase (AOTCase,[1] EC 2.1.3.9) was recently discovered to be part of a novel arginine biosynthesis pathway in plant pathogens of the Xanthomonadaceae family such as *Xylella* and *Xanthomonas* (*17*−*19*). These pathogens attack a variety of economically important crops, including citrus fruits, cotton, tomatoes, and rice (*20*, *21*). Genome sequence analyses showed that an AOTCase-like gene is also present in some human pathogens such as *Stenotrophomonas maltophilia* and members of the genus *Bacteroides* (*22*). In the case of *Bacteroides fragilis*, this gene was later confirmed to encode another novel transcarbamylase, *N*-succinyl-L-ornithine transcarbamylase (SOTCase, EC 2.1.3.11) (*23*). Crystal structures of both AOTCase and SOTCase bound with substrate or substrate analogues have recently been determined (*17*, *18*, *23*). An extended density at the side chain tip of Lys302 in AOTCase was observed, suggesting a post-translational modification. Because Lys302 is located within the active site of AOTCase and is not present in SOTCase, it was proposed as one of

[†]This work was supported by Public Health Service Grants DK-47870 (M.T.) and DK-067935 (D.S.) from the National Institute of Diabetes and Digestive and Kidney Diseases. J.H. was supported by a scholarship from the Doug and Lynn Parsons Family Foundation.

*To whom correspondence should be addressed. E-mail: dshi@cnmcresearch.org. Phone: (202) 476-5817. Fax: (202) 476-6014.

[1]Abbreviations: ACIT, *N*-acetyl-L-citrulline; ANOR, *N*-acetyl-L-norvaline; AORN, *N*-acetyl-L-ornithine; AOTCase, *N*-acetyl-L-ornithine transcarbamylase; ATCase, aspartate transcarbamylase; OTCase, ornithine transcarbamylase; CP, carbamyl phosphate; ORN, L-ornithine; PALAO, N^{δ}-(phosphonoacetyl)-N^{α}-acetyl-L-ornithine; rmsd, root-mean-square deviation; SORN, *N*-succinyl-L-ornithine; WT, wild-type; *xc*, *Xanthomonas campestris*.

Published on Web 07/14/2010

Table 1: Data Collection and Refinement Statistics[a]

	PALAO	K302A	K302E	K302R
		Data Collection		
space group	$I2_13$	$I2_13$	$I2_13$	$I2_13$
resolution (Å)	2.2	1.9	1.85	2.2
unit cell parameters (Å)	$a = b = c = 128.88$	$a = b = c = 128.92$	$a = b = c = 129.29$	$a = b = c = 127.39$
no. of measurements	219475	305757	390128	246817
no. of unique reflections	18269 (1832)	28236 (1365)	30622 (1456)	17635 (879)
redundancy	12.0 (11.8)	10.8 (5.4)	12.8 (5.4)	14.0 (13.1)
completeness (%)	99.8 (100.0)	100.0 (100.0)	99.7 (95.1)	100.0 (100.0)
$\langle I/\sigma(I)\rangle$	15.0 (4.9)	16.4 (2.3)	19.8 (2.8)	8.7 (3.7)
R_{merg}[b]	7.4 (48.4)	6.5 (64.9)	5.2 (55.3)	9.8 (79.1)
Wilson B (Å^2)	30.4	27.6	28.6	21.9
		Refinement		
resolution range (Å)	50.0−2.2	50−1.9	50−1.85	50−2.2
no. of protein atoms	2620	2613	2617	2619
no. of water atoms	90	219	193	146
no. of hetero atoms	24	24	24	24
rmsd for bond lengths (Å)	0.006	0.005	0.005	0.005
rmsd for bond angles (deg)	1.1	1.2	1.2	1.2
R_{work} (%)[c]	20.0	19.8	20.0	18.9
R_{free} (%)[d]	24.3	23.2	23.2	22.2
average B factor (Å^2)	41.7	32.2	32.3	35.3

[a]Figures in parentheses apply to the highest-resolution shell. [b]$R_{merg} = \sum_h\sum_i|I(h,i) - \langle I(h)\rangle|/\sum_h\sum_i I(h,i)$, where $I(h,i)$ is the intensity of the ith observation of reflection h and $\langle I(h)\rangle$ is the average intensity of redundant measurements of reflection h. [c]$R_{work} = \sum_h||F_{obs}| - |F_{calc}||/\sum_h|F_{obs}|$. [d]$R_{free} = \sum_h||F_{obs}| - |F_{calc}||/\sum_h|F_{obs}|$ for 5% of the reserved reflections.

three key signature residues to distinguish the two carbamylases (*22*). Here, we demonstrate that Lys302 is post-translationally modified by carboxylation and that this change affects the catalytic function of the enzyme.

MATERIALS AND METHODS

Materials. All chemicals were purchased from Sigma Chemical Co. unless otherwise specified. ANOR was purchased from Indofine Chemical Co., Inc. *N*-Acetyl-L-citrulline was custom synthesized and purified by Chiral Quest Co. PALAO (> 95% pure) was synthesized by IMI TAMI Institute of Research and Development Ltd. (*19*). *xc*AOTCase was prepared and purified as previously described (*18*). Mutants K302A (primer, 5′-CTGCGTCGCAACGTC**GCG**GCTACTGATGCGGTG-3′), K302E (primer, 5′-CTGCGTCGCAACGTC**GAG**GCTACTGATGCGGTG-3′), and K302R (primer, 5′-CTGCGTCGCAACGTC**AGG**GCTACTGATGCGGTG-3′) were generated by site-directed mutagenesis using the "Quik Change" mutagenesis kit (Stratagene) according to the manufacturer's protocol. The correct mutants were confirmed by DNA sequencing. Recombinant mutant proteins were expressed and purified in the same manner as the wild-type enzyme.

Activity Assay. The modified colorimetric assay method, which detects the formation of the ureido group during the transcarbamylation reaction (*24*), was used to measure enzyme activity. CP and AORN concentrations were kept constant at 4.0 mM. After incubation for 5 min, the reaction was stopped by the addition of 1 mL of color reagent, as described previously (*19*). A set of tubes containing known amounts of *N*-acetyl-L-citrulline was included with each rack of enzyme assays to produce a standard curve for calculation of the enzyme specific activity.

Mass Spectrometric Analysis. To identify the post-translational modification, mass spectrometric analysis was conducted on a 4700 ABI TOF/TOF mass spectrometer (Applier Biosystems) based on the method described previously (*25*). In brief, 10 μg of native protein was digested overnight at 310 K using trypsin in 50 mM ammonium bicarbonate (pH 7.4). After being desalted using a C18 ZipTip micropipet tip, the resulting peptides were eluted in 10 μL of an acetonitrile/0.1% TFA mixture [70:30 (v:v)]. The sample was mixed with matrix solution and spotted on a MALDI plate to be subjected to mass spectrometric analysis.

Chemical Rescue Experiments. The assay in the presence of various selected chemicals was conducted as described above. The stock solutions of small chemicals were titrated to the pH of the assay with KOH or HCl.

^{13}C NMR Experiments. The wild type and the K302A mutant protein of AOTCase (~10 mg) were precipitated by degassed buffer (pH 4.5) containing 25 mM sodium acetate. After centrifugation, the precipitate was redissolved by addition of a buffer containing 20 mM $NaH^{13}CO_3$, 100 mM Tris-HCl (pH 8.0), and 50 mM NaCl. Before NMR experiments, 40 μL of D_2O was added to 500 μL of the protein sample. The ^{13}C NMR spectra were recorded on a Bruker Avance 600 spectrometer (operating at 14.1 T) equipped with a direct ^{13}C detection probe at 298 K. The experimental settings and processing parameters for the wild-type protein and K302A variant were identical; 512 transients were collected with 4K time domain points and a spectral width of 3019 Hz centered at 160 ppm. The spectra were processed using exponential multiplication with the line broadening factor set to 3 Hz. The similarity of the protein concentration in both samples was verified by ^1H NMR (not shown).

Crystallization, Data Collection, and Processing. PALAO-bound wild-type and mutant AOTCase crystals were grown using the hanging drop vapor diffusion method, with conditions similar to those used to produce native and ligand-complexed AOTCase crystals (*18*, *23*); 2.0 μL of an ~10 mg/mL solution of AOTCase was mixed with 1.6 μL of a reservoir solution and 0.4 μL of a PALAO solution (~0.01 M). The reservoir solution

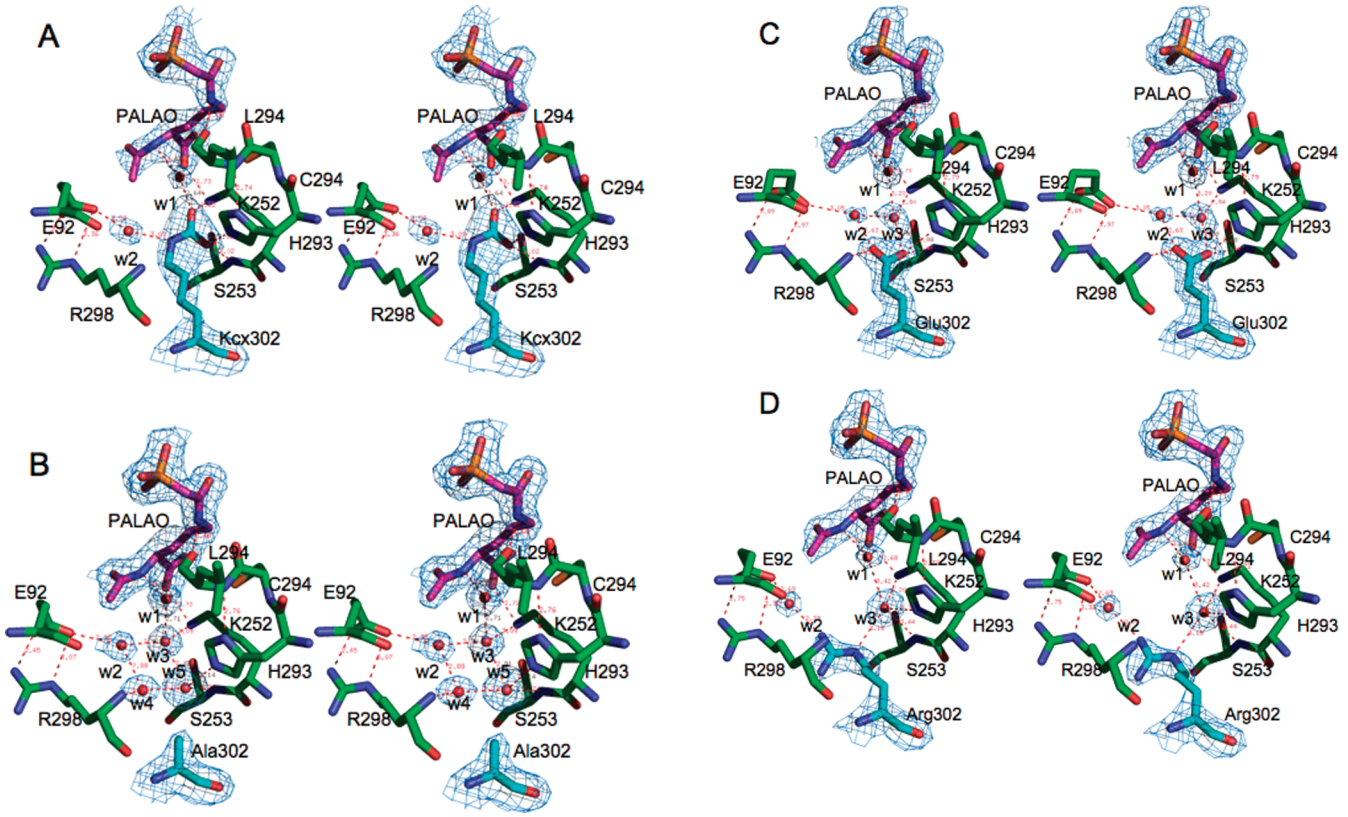

FIGURE 1: Stereoview of the structure and hydrogen bonding network surrounding residue 302. (A) PALAO-bound wild-type AOTCase, (B) PALAO-bound K302A AOTCase, (C) PALAO-bound K302E AOTCase, and (D) PALAO-bound K302R AOTCase. Contours of the electron density maps ($2F_o - F_c$) around PALAO, residue 302, and water molecules are shown as a brown cage at 1.0σ. The final refined positions of the ligands and surrounding protein residues are represented as colored sticks. The predicted hydrogen bonding interactions are represented as pink dashed lines. The water molecules are represented as pink spheres. The carbon of PALAO, residue 302, and other protein residues are shown with pink, light blue, and green sticks, respectively.

contained 20% (w/v) PEG 3350, 0.2 M lithium sulfate, and 0.1 M bis-Tris (pH 6.0). Diffraction data for the PALAO-bound crystal were recorded at 100 K at beamline F1 of the Cornell High Energy Synchrotron Source. Data sets for the PALAO-bound mutant AOTCase crystals were obtained using a Rigaku anode X-ray generator in the Molecular Structure Section of the National Institutes of Health. All data were processed using HKL2000 (*26*) and reduced using the program TRUNCATE in the CCP4 suite (*27*). Data collection parameters are listed in Table 1.

Structure Solution and Refinement. Molecular replacement was used for phase determination of the PALAO-bound wild-type and mutant AOTCase structures. The coordinates of AOTCase (Protein Data Bank entry 3KZO) after removal of ligands or water molecules were used for phase determination. Upon rigid-body refinement, electron density corresponding to the ligands could be clearly visualized. The ligands were built into the map using O (*28*). Refinements were conducted using molecular annealing, energy minimization, and restrained *B* factor refinement with CNS1.1 (*29*). During refinements, 5% of the reflections at various resolutions were randomly selected to be set aside to calculate R_{free} to monitor the progress of refinement (*30*). After every cycle of refinement, the model was manually adjusted using O (*28*). Water molecules were automatically assigned using the program WATERPICK of CNS. Model quality was checked using PROCHECK (*31*) to ensure good stereochemistry for all three models. The final refinement statistics are listed in Table 1.

Figure 1 was drawn using Pymol (http://www.pymol.org). Figure 3 was drawn using ChemDraw 8.0. The coordinates have been deposited with the RCSB Protein Data Bank (PDB) as entries 3M4J, 3M4N, 3M5C, and 3M5D.

RESULTS

Lys302 in AOTCase Is Carboxylated. To investigate the nature of the modification of Lys302 and how it affects catalytic activity, we revisited all AOTCase structures. In the PALAO-bound AOTCase structure, the electron density map clearly indicates that Lys302 is post-translationally modified (Figure 1A). The type of modification can include methylation, acetylation, carbamylation, and carboxylation. The shape of the electron density can been used to distinguish methyl groups from larger functional groups, but it is difficult to distinguish among acetyl, carbamyl, and carboxyl groups, all of which have three non-hydrogen atoms in a plane. Given the hydrogen bonding network with surrounding residues [Lys252, Ser253, and His293 (Table 2)], a carboxylated modification is the most likely choice for the modification of Lys302 in AOTCase. To exclude the possibility that the modification's identity represents chemically stable moieties (methyl, acetyl, and carbamyl), we analyzed trypsin-digested fragments of purified AOTCase by TOF-TOF mass spectroscopy. As expected, only a peptide fragment with an unmodified Lys302 was observed, consistent with the lability of the carboxylic group in acidic solutions. At low pH, the carboxyl group is spontaneously released as carbon dioxide (*14*, *32*), in contrast to other modified groups that are stably bound and can be observed by mass spectrometry analysis after proteolysis (*33*).

The putative carboxyl group on the modified Lys302 forms direct hydrogen bonds with main chain or side chain nitrogen

atoms of Lys252, Ser253, and His293 (Figure 1A and Table 2). Among these, Lys252 is involved in direct hydrogen bonding to the carboxyl group of the AORN moiety of PALAO, and His293 forms a strong hydrogen bond with the main chain nitrogen atom of Leu295 in the conserved His293-Cys294-Leu295-Pro206 (HCLP) motif. The hydrogen bonding network among the carboxyl group of modified Lys302, His293, and the main chain nitrogen atom of Leu295 is reminiscent of the similar hydrogen bonding network, Glu310-His302-Leu304 and Glu299-Leu272-Leu274, found in human and *Escherichia coli* OTCase, respectively (*34*, *35*). These three residues are conserved in all OTCase sequences, and the interactions between them are important for maintaining the HCLP motif in a specific conformation to orient their main chain oxygen atoms toward the active site. In all known transcarbamylase structures, a leucine residue corresponding to Leu295 is in an energetically unfavorable conformation and the peptide bond between this leucine and Pro296 is in the cis conformation. In addition to the direct hydrogen bonding interaction described above, the carboxyl group on the modified Lys302 interacts with the α-amino nitrogen atom of the AORN moiety of PALAO and Glu92 from the adjacent subunit via water molecules.

Table 2: Interactions between Carboxylated Lysine and Other Residues at the Active Site of AOTCase

		bound ligands				
Kcx302	other residues	PALAO	CP[a]	AORN[b]	CP and ANOR[c]	SO_4 and ACIT[d]
OQ1	K252 NZ	2.6	2.6	2.7	2.6	2.6
OQ1	w1[e]	2.6		2.6	2.6	2.7
OQ2	S253 N	3.0	3.1	2.8	2.9	2.9
OQ2	H293 NE2	3.0	3.2	3.0	2.9	2.9
NZ	w2[f]	3.1		2.9	3.0	3.0

[a]The values were calculated on the basis of PDB entry 3KZM. [b]The values were calculated on the basis of PDB entry 3KZN. [c]The values were calculated on the basis of PDB entry 3KZO. [d]The values were calculated on the basis of PDB entry 3KZK. [e]This water molecule forms a hydrogen bond to the N1 atom of PALAO, AORN, or ANOR and the backbone O atom of Pro296 as well. [f]This water molecule forms a hydrogen bond to the OE1 atom of Glu92 from the adjacent subunit as well.

When we revisited all previously determined AOTCase structures (see Figure S1 of the Supporting Information) we found the following. (1) Lys302 was carboxylated in the absence of substrate binding, but substrate binding immobilizes the side chain of Lys302 further by hydrogen bonding interaction via water molecules. (2) Water-mediated hydrogen bonding promotes interactions of carboxylated Lys302 with Glu92 from the adjacent subunit and the α-amino nitrogen atom of AORN. (3) As in AOTCase, in the structure of the SOTCase E92Z (Z = Ala, Ser, Pro, or Val) mutant with *N*-succinyl-L-norvaline bound (*22*), the carboxylated Lys302 forms a hydrogen bond to the α-amino nitrogen atom and the succinyl carboxyl group of *N*-succinyl-L-norvaline via water molecules (Figure S1 of the Supporting Information).

To obtain direct, independent evidence of the carboxylation of Lys302, ^{13}C NMR experiments were conducted with both the wild-type protein and the K302A mutant. As observed for other proteins with carboxylated lysine (*36*, *37*), the strong ^{13}C NMR signal at 164 ppm characteristic of a carboxyl group was clearly detectable in AOTCase wild-type protein labeled with [^{13}C]bicarbonate, in contrast to the K302A mutant for which the signal was weak (Figure 2). Because there are 17 other lysine residues in the protein, the weak signal seen for the K302A mutant might be caused by the adventitious carboxylation of another lysine with a reduced pK_a, which has been observed for the K392A mutant of the sensor domain of the BlaR protein (*38*).

Functional and Structural Studies of Lys302 Mutants. To investigate the effect of lysine carboxylation on enzyme activity, Lys302 was mutated to alanine, glutamate, or arginine.

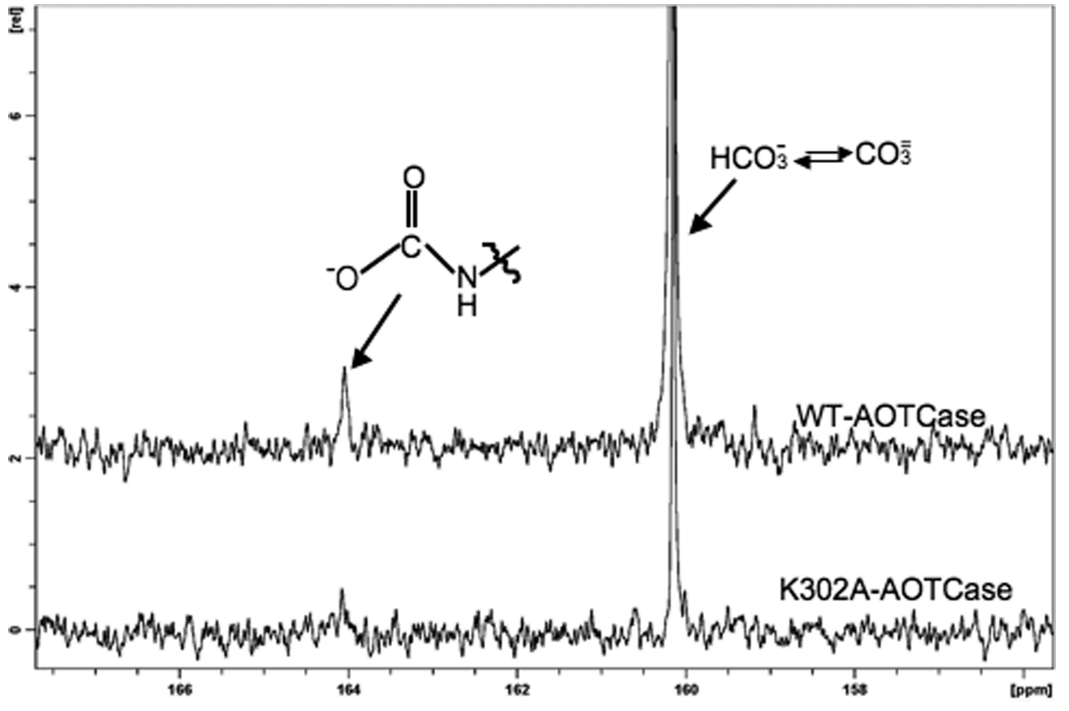

FIGURE 2: ^{13}C NMR spectra of wild-type (top) and K302A mutant (bottom) AOTCase (1 mM). Experiments were performed in 100 mM Tris-HCl, 50 mM NaCl, and 7% D_2O (pH 8.0), supplemented with 20 mM $NaH^{13}CO_3$. The position of the resonance attributed to carboxylated lysine in the enzyme is around 164 ppm.

Table 3: Specific Activities[a] of Wild-Type and Mutant AOTCase in the Presence of Acids (0.5 M)

	specific activity (μmol min^{-1} mg^{-1})			
addition	wild type	K302A	K302E	K302R
none	43.4 ± 0.4	23.0 ± 0.5	7.1 ± 0.1	0.059 ± 0.01
formate	44.1 ± 1.2	26.4 ± 0.6	6.7 ± 0.2	0.093 ± 0.01
acetate	48.5 ± 1.1	21.2 ± 0.8	6.6 ± 0.5	0.104 ± 0.03

[a]The means ± standard deviation are shown (n = 3).

Each of these variants was expressed in *E. coli* and gave similar yields. Enzymatic assays demonstrated a significant decrease in enzymatic activity in all three mutants, reflecting the functional importance of Lys302 (Table 3). The order of the level of enzymatic activity for the wild-type (WT) and three mutants was as follows: WT > K302A > K302E ≫ K302R. To determine the structural basis of these results, the WT and mutant enzymes bound with PALAO were crystallized and their structures were determined at 1.8−2.2 Å resolution. Only the K302R mutation had an appreciable effect on the structure of the protein. Because K302 is located near the AORN binding site, the mutations would weaken binding of AORN to the active site.

In the structure of the K302A mutant, three additional water molecules (labeled w3−w5 in Figure 1B) replace the carboxylated lysine. The two water molecules (labeled w1 and w2 in Figure 1A−D) that mediate the hydrogen bonding interaction of carboxylated Lys302 with PALAO and Glu92 from the adjacent subunit are also found in the K302A mutant structure. Furthermore, these water molecules maintain a hydrogen bonding network similar to that of the wild-type enzyme. These results might explain why the K302A mutant retains significant catalytic activity (Table 3). To investigate whether adding short chain carboxylic acids to the K302A mutant increases its activity as in other enzymes (*14*, *15*, *39*, *40*), the activity of the K302A mutant was measured in the presence of high formate and acetate concentrations (0.5 M). Surprisingly, the activity of the K302A mutant was not significantly improved. The crystal structure of the K302A mutant being soaked in the crystallization buffer in the presence of 0.5 M acetate was also determined (not shown), and we observed that the same five water molecules were present in the cavity that replaced the side chain of the carboxylated lysine. This, the acetate's inability to replace the water molecules in the crystal structure, is consistent with the unchanged activity assay results.

The side chain of Glu302 in the K302E mutant structure is well-defined and anchored by hydrogen bonding interaction with the main chain nitrogen atom of Arg298 and weakly hydrogen bonded to the main chain nitrogen atom of Ser253 (Figure 1C). Two of three additional water molecules (w4 and w5) observed in the K302A mutant structure occupied the same position as the carboxyl oxygen atoms of Glu302 and form a similar hydrogen bonding network. Relative to the PALAO-bound wild-type structure, there is only one more water molecule (w3) at the position of the carboxyl group of the carboxylated Lys302. This water molecule mediates a hydrogen bonding interaction between Glu302 and Lys252. Two common water molecules (w1 and w2) that interact with PALAO and Glu92 from the adjacent subunit, respectively, were also identified in the K302E structure.

Our observation that the K302E mutant had lower enzymatic activity than the K302A mutant (Table 3) was surprising because the carboxyl group of the glutamate could conceivably function like a carboxylated lysine. The explanation may be that, in the K302A mutant, the hydrogen bonding network is well-maintained by water molecules in the cavity that replaces the carboxylated lysine. In particular, w3 is optimally located for strong hydrogen bonding to w1 (2.7 Å), which in turn binds AORN. The distances between w1 and the carboxyl oxygen of carboxylated Lys302 in all wild-type crystal structures are within 2.4−2.7 Å, but the distance between w1 and w2 in the K302E structure is significantly greater (3.2 Å). The weaker hydrogen bonding interaction may be a reason for the lower enzymatic activity of the K302E mutant.

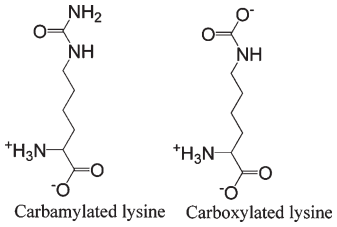

FIGURE 3: Chemical structure of carbamylated vs carboxylated lysine.

In contrast to the K302A and K302E structures, the K302R structure shows a much larger reduction in enzyme activity relative to the wild-type enzyme. The electron density for the side chain of Arg302 is weak, and the temperature factor of its side chain is 54.4 Å^2, significantly higher than those of carboxylated Lys302 (44.7 Å^2) and Glu302 (33.4 Å^2), implying greater flexibility. Furthermore, the side chain of Arg302 is oriented differently from the carboxyl group of carboxylated Lys302 and pushes the nearby residues His180, Pro181, and Lys182 outward ~1.0 Å (Figure 1D). However, the water molecules involved in hydrogen bonding to the α-amino nitrogen atom of PALAO (w1) and the side chains of Lys252 (w3) and Glu92 (w2) from the adjacent subunit are conserved. Consistent with the K302E structure, the distance between w1 and w2 is even greater (3.4 Å) than in the WT structure, and the hydrogen bonding interaction between w2 and w3 is no longer observed. Thus, the almost undetectable enzymatic activity of the K302R mutant probably results from the changes at its active site, including the weakened hydrogen bonding network involved in substrate binding.

DISCUSSION

Several lines of evidence clearly indicate that Lys302 in AOTCase is carboxylated. First, the extra electron density indicates that the side chain of Lys302 is modified. Second, the hydrogen bonding environment of Lys302 for hydrogen bonding interactions is compatible with a carboxyl group, but not for a positively charged lysine side chain. Third, the modification is labile at low pH, since mass spectroscopy of samples prepared at low pH indicated that Lys302 was no longer modified. Fourth, the clear presence of the indicative ^{13}C NMR signal at 164 ppm for wild-type protein and its absence in the K302A mutant confirm the carboxylation of Lys302.

It is well-known that lysine carboxylation is nonenzymatic and reversible, while other post-translational modifications such as methylation, acetylation, and carbamylation are irreversible and can be detected by mass spectroscopy. Furthermore, lysine methylation and acetylation usually require an enzyme-catalyzed reaction in vivo (*41*). Therefore, it is unlikely that such lysine modifications will be observed in recombinant proteins overexpressed in a foreign host (e.g., *E. coli*). Lysine methylation can be achieved by using special chemicals in vitro, but these chemicals are not present in vivo. Lysine carbamylation and carboxylation use

Table 4: Protein Structures with Lysine Carboxylation Modification

PDB entry	enzyme name	residue	organism source	function
2OGJ	dihydroorotase	175	*Agrobacterium tumefaciens*	bridging two Zn(II)
2Z26	dihydroorotase	102	*E. coli*	bridging two Zn(II)
3JZE	dihydroorotase	103	*Salmonella enterica*	bridging two Zn(II)
2GWN	dihydroorotase	149	*Porphyromonas gingivalis*	bridging two Zn(II)
3F4C	organophosphorus hydrolase	243	*Geobacillus stearothermophilus*	bridging two Co(II)
3ICJ	metal-dependent hydrolase	294	*Pyrococcus furiosus*	bridging two Zn(II)
3GTX	organophosphorus hydrolase	243	*Deinococcus radiodurans*	bridging two Co(II)
2QPX	metal-dependent hydrolase	166	*Lactobacillus casei*	bridging two Zn(II)
2FTW	dihydropyrimidinase	158	*Dictyostelium discoideum*	bridging two Zn(II)
2FVK	dihydropyrimidinase	167	*Saccharomyces kluyveri*	bridging two Zn(II)
3DC8	dihydropyrimidinase	147	*Sinorhizobium meliloti*	bridging two Zn(II)
3GNH	L-Lys/Arg carboxypeptidase	211	*Caulobacter crescentus* cb15	bridging two Zn(II)
3DUG	arginine carboxypeptidase	182	unidentified	bridging two Zn(II)
2VC7	phosphotriesterase	137	*Solfolobus solfataricus*	bridging two Co(II)
2R1N	metallophosphotriesterases	169	*A. tumefaciens*	bridging two Co(II)
2OB3	phosphotriesterase	169	*Brevundimonas diminuta*	bridging two Zn(II)
3E74	allantoinase	146	*E. coli*	bridging two Fe(III)
1EJX	urease	217	*Klebsiella aerogenes*	bridging two Ni(II)
1E9Z	urease	219	*Helicobacter pylori*	bridging two Ni(II)
4UBP	urease	220	*Bacillus pasteurii*	bridging two Ni(II)
1ONW	isoaspartyl dipeptidase	162	*E. coli*	bridging two Zn(II)
1K1D	D-hydanroinase	150	*G. stearothermophilus*	bridging two Zn(II)
1GKR	L-hydanroinase	147	*Arthrobacter aurescens*	bridging two Zn(II)
1GKP	D-hydanroinase	150	*Thermus* sp.	bridging two Zn(II)
1NFG	D-hydantoinase	148	*Ralstonia pickettii*	bridging two Zn(II)
2ICS	adenine deaminase	154	*Enterococcus faecalis*	bridging two Zn(II)
1RQB	transcarboxylase	184	*Propionibacterium freudenreichii*	binding one Co(II)
2QF7	pyruvate carboxylase	718	*Rhizobium etli*	binding one Zn(II)
3BG3	pyruvate carboxylase	741	*Homo sapiens*	binding one Mn(II)
2OEM	Rubisco-like protein	173	*Geobacillus kaustophilus*	binding one Mg(II)
1WDD	Rubisco	201	*Oryza sativa*	binding one Mg(II)
1GK8	Rubisco	201	*Chlamydomonas reinhardtii*	binding one Mg(II)
1BWV	Rubisco	201	*Galdieria partita*	binding one Mg(II)
2WTZ	ATP-dependent MurE ligase	262	*Mycobacterium tuberculosis*	binding one Mg(II)
2JFG	MurD ligase	198	*E. coli*	catalytic role?
1E8C	MurE ligase	224	*E. coli*	catalytic role?
1JBW	folypolyglutamate synthetase	185	*L. casei*	catalytic role?
1W78	FolC bifunctional protein	188	*E. coli*	binding one Mg(II)
3HBR	OXA-48 β-lactamase	73	*Klebsiella pneumoniae*	catalytic role
3ISG	class D β-lactamase	70	*E. coli*	catalytic role
2P9V	AmpC β-lactamase	315	*E. coli*	catalytic role
1K55	OXA-10 β-lactamase	70	*Pseudomonas aeruginosa*	catalytic role
1K38	β-lactamase OXA-2	70	*Salmonella typhimurium*	catalytic role
1XQL	alanine racemase	129	*G. stearothermophilus*	binding substrate?
1VFS	alanine racemase	129	*Streptomyces lavendulae*	binding substrate?
1RCQ	alanine racemase	122	*P. aeruginosa*	binding substrate?
2J6V	UV damage endonuclease	229	*Thermus thermophilus*	catalytic role
1H01	cell division protein kinase 2	33	*H. sapiens*	catalytic role?
2UYN	protein TdcF	A58	*E. coli*	structural role?
1HL9	fucosidase	338	*Thermotoga maritima*	structural role?
1PU6	3-methyladenine DNA glycosylase	205	*H. pylori*	structural role?

completely different mechanisms to form functionally different groups (Figure 3). Carbamylation can be achieved by cyanate produced from myeloperoxidase-catalyzed oxidation of thiocyanate, an anion abundant in plasma and increased in smokers, or from urea in the plasma. Lysine carboxylation, on the other hand, occurs readily in aqueous solution in the presence of carbon dioxide at a basic pH (*32*, *42*). Even though carbamylation and carboxylation use very different mechanisms, the two are confused in the literature. Lysine carbamylation (or carbamoylation) is mentioned in several publications (*15*, *32*, *42*−*44*), when the actual reaction is in fact carboxylation.

The activity of the K302A mutant is almost half of that of the wild-type enzyme, raising the question of why AOTCase retains a lysine at this position. Perhaps this lysine was maintained through evolution to distinguish AOTCase from SOTCase which uses *N*-succinyl-L-ornithine (SORN) rather than AORN (*22*), and OTCase which uses L-ornithine. An alternative explanation may be found in the very low activity of the K302R mutant. The side chain of arginine has a positive charge, while carboxylated lysine has a negative charge. The side chain of unmodified lysine is usually located in a position similar to that of arginine, as observed in the structure of UV damage endonuclease (*14*). It would be expected that the activity of AOTCase with an uncarboxylated lysine would be as low as that of the K302R mutant. It could further be surmised that the respective organisms need to use carboxylation as a switch to turn "on" or "off" the arginine biosynthetic

pathway. It has been well-known that rubulose-1,5-bisphosphate carboxylase/oxygenase (Rubisco) in plant cells uses the carboxylation of Lys201 as a switch to turn the enzyme on during the day and off at night by removing the carboxyl group (*45*, *46*). Carbon dioxide and bicarbonate have been found to play an important biological role in modulating several biological processes, including photosynthetic carbon fixation (*47*), pH homeostasis (*48*), carbon metabolism (*49*), activation of virulence in pathogenic organisms (*50*), sperm maturation (*51*), stimulation of mammalian G-protein-responsive adenylyl cyclase (*52*), and an alarmone in *Drosophila* (*53*, *54*). Whether carboxylation of a key lysine in their related proteins is used as an underlying regulatory mechanism should be investigated further.

There are 197 structures with a carboxylated lysine residue (modified residue indicated as Kcx) in the PDB. If structures that are 90% identical are counted only once, there are still 52 unique structures remaining in this pool (Table 4). These proteins include hydantoinase (*40*, *55*), folylpolyglutamate synthase (*43*), UV damage endonuclease (*14*), OXA10, OXA-1 class D β-lactamase (*38*, *56*, *57*), urease (*42*), phosphotriesterase (*58*), dihydroorotase (*59*), dihydropyrimidinase (*60*), organophosphate hydrolase (*61*), and MurE and MurD ligases (*44*, *62*). In most of these proteins, the carboxylated lysine bridges two metal ions, similar to the role of glutamate or aspartate in proteins with two metal-binding sites (26 structures among 52). However, the urease apoenzyme can be activated in vitro only in the presence of carbon dioxide prior to nickel binding (*63*), suggesting that the carboxylated lysine may have other structural roles beyond binding metals. In some proteins such as β-lactamase, UV damage endonuclease, Rubisco, MurD and MurE ligase, and BlaR signal transducer protein, a carboxylated lysine plays an essential catalytic role. More interestingly, in three structures (PDB entries 1HL9, 1PU6, and 2UYN for fucosiadase, 3-methyladenine DNA glycosylase, and TdcF protein of unknown function, respectively), the carboxylated lysines are located near the surface of proteins, presumably playing primarily a structure stabilizing role (*64*−*66*). Because the carboxyl group is labile at acidic pH but easily formed in the presence of carbon dioxide at basic pH, the number of proteins with lysine carboxylation must be underestimated. Furthermore, the carboxylated lysine must be fixed in place by metal ions (either one or two) or hydrogen bonding with other protein residues (at least one). Therefore, any detection method involving denaturing the proteins will result in release of the carboxyl group. With current technology, ^{13}C NMR (*38*) and crystallography are the only methods that can detect this modification. However, these methods are not amenable to high-throughput investigations. The majority (49 of 52 structures in the PDB) of known lysine carboxylation modifications were found to be located at or near the active site, probably because these sites receive the most attention. Revisiting the structures in PDB with more attention to surface lysines might reveal more structures with carboxylated lysines.

In conclusion, we have shown that Lys302 in AOTCase is post-translationally modified by carboxylation and that this modification may be functionally important for enzymatic activity. Lysine carboxylation is likely to be a more common event than currently appreciated and may play a critical role in enzymatic activity and protein stability.

ACKNOWLEDGMENT

We thank Dr. David Davies for facilitating our use of the diffraction equipment in the Molecular Structure Section of the National Institutes of Health, Dr. Fred Dyda for help in data collection and processing, and Dr. Yui-Fai Lam at the University of Maryland for help in setting up NMR measurements. The Cornell High Energy Synchrotron Source (CHESS) is supported by National Science Foundation Granr DMR 0225180, and the Macromolecular Diffraction Facility at CHESS (MacCHESS) is supported by Grant RR-01646 from the National Institutes of Health, through its National Center for Research Resources.

SUPPORTING INFORMATION AVAILABLE

Structure and hydrogen bonding network around residue 302 for previously determined AOTCase structures (Figure S1). This material is available free of charge via the Internet at http://pubs.acs.org.

REFERENCES

1. Close, P., Creppe, C., Gillard, M., Ladang, A., Chapelle, J. P., Nguyen, L., and Chariot, A. (2010) The emerging role of lysine acetylation of non-nuclear proteins. *Cell. Mol. Life Sci. 67*, 1255–1264.
2. Geiman, T. M., and Robertson, K. D. (2002) Chromatin remodeling, histone modifications, and DNA methylation-how does it all fit together? *J. Cell. Biochem. 87*, 117–125.
3. An, W. (2007) Histone acetylation and methylation: Combinatorial players for transcriptional regulation. *Subcell. Biochem. 41*, 351–369.
4. Yang, F., Bian, C., Zhu, L., Zhao, G., Huang, Z., and Huang, M. (2007) Effect of human serum albumin on drug metabolism: Structural evidence of esterase activity of human serum albumin. *J. Struct. Biol. 157*, 348–355.
5. Xu, A. S., Labotka, R. J., and London, R. E. (1999) Acetylation of human hemoglobin by methyl acetylphosphate. Evidence of broad regio-selectivity revealed by NMR studies. *J. Biol. Chem. 274*, 26629–26632.
6. Ueno, H., Pospischil, M. A., and Manning, J. M. (1989) Methyl acetyl phosphate as a covalent probe for anion-binding sites in human and bovine hemoglobins. *J. Biol. Chem. 264*, 12344–12351.
7. Stavropoulos, P., Nagy, V., Blobel, G., and Hoelz, A. (2008) Molecular basis for the autoregulation of the protein acetyl transferase Rtt109. *Proc. Natl. Acad. Sci. U.S.A. 105*, 12236–12241.
8. Bewley, M. C., Graziano, V., Jiang, J., Matz, E., Studier, F. W., Pegg, A. E., Coleman, C. S., and Flanagan, J. M. (2006) Structures of wild-type and mutant human spermidine/spermine N1-acetyltransferase, a potential therapeutic drug target. *Proc. Natl. Acad. Sci. U.S.A. 103*, 2063–2068.
9. Walter, T. S., Meier, C., Assenberg, R., Au, K. F., Ren, J., Verma, A., Nettleship, J. E., Owens, R. J., Stuart, D. I., and Grimes, J. M. (2006) Lysine methylation as a routine rescue strategy for protein crystallization. *Structure 14*, 1617–1622.
10. Stark, G. R., Stein, W. H., and Moore, S. (1960) Reactions of the cyanante present in aqueous urea with amino acids and proteins. *J. Biol. Chem. 235*, 3177–3181.
11. Bobb, D., and Hofstee, B. H. (1971) Gel isoelectric focusing for following the successive carbamylations of amino groups in chymotrypsinogen A. *Anal. Biochem. 40*, 209–217.
12. Kraus, L. M., and Kraus, A. P., Jr. (2001) Carbamoylation of amino acids and proteins in uremia. *Kidney Int., Suppl. 78*, S102–S107.
13. Al-Dirbashi, O. Y., Al-Hassnan, Z. N., and Rashed, M. S. (2006) Determination of homocitrulline in urine of patients with HHH syndrome by liquid chromatography tandem mass spectrometry. *Anal. Bioanal. Chem. 386*, 2013–2017.
14. Meulenbroek, E. M., Paspaleva, K., Thomassen, E. A., Abrahams, J. P., Goosen, N., and Pannu, N. S. (2009) Involvement of a carboxylated lysine in UV damage endonuclease. *Protein Sci. 18*, 549–558.
15. Dementin, S., Bouhss, A., Auger, G., Parquet, C., Mengin-Lecreulx, D., Dideberg, O., van Heijenoort, J., and Blanot, D. (2001) Evidence of a functional requirement for a carbamoylated lysine residue in MurD, MurE and MurF synthetases as established by chemical rescue experiments. *Eur. J. Biochem. 268*, 5800–5807.
16. Cha, J., and Mobashery, S. (2007) Lysine N^{ζ}-decarboxylation in the BlaR1 protein from *Staphylococcus aureus* at the root of its function as an antibiotic sensor. *J. Am. Chem. Soc. 129*, 3834–3835.
17. Shi, D., Yu, X., Roth, L., Morizono, H., Tuchman, M., and Allewell, N. M. (2006) Structures of N-acetylornithine transcarbamoylase from *Xanthomonas campestris* complexed with substrates and substrate analogs imply mechanisms for substrate binding and catalysis. *Proteins 64*, 532–542.

18. Shi, D., Morizono, H., Yu, X., Roth, L., Caldovic, L., Allewell, N. M., Malamy, M. H., and Tuchman, M. (2005) Crystal structure of N-acetylornithine transcarbamylase from *Xanthomonas campestris*: A novel enzyme in a new arginine biosynthetic pathway found in several eubacteria. *J. Biol. Chem. 280*, 14366–14369.
19. Morizono, H., Cabrera-Luque, J., Shi, D., Gallegos, R., Yamaguchi, S., Yu, X., Allewell, N. M., Malamy, M. H., and Tuchman, M. (2006) Acetylornithine transcarbamylase: A novel enzyme in arginine biosynthesis. *J. Bacteriol. 188*, 2974–2982.
20. da Silva, F. R., Vettore, A. L., Kemper, E. L., Leite, A., and Arruda, P. (2001) Fastidian gum: The *Xylella fastidiosa* exopolysaccharide possibly involved in bacterial pathogenicity. *FEMS Microbiol. Lett. 203*, 165–171.
21. da Silva, A. C., Ferro, J. A., Reinach, F. C., Farah, C. S., Furlan, L. R., Quaggio, R. B., Monteiro-Vitorello, C. B., Van Sluys, M. A., Almeida, N. F., Alves, L. M., do Amaral, A. M., Bertolini, M. C., Camargo, L. E., Camarotte, G., Cannavan, F., Cardozo, J., Chambergo, F., Ciapina, L. P., Cicarelli, R. M., Coutinho, L. L., Cursino-Santos, J. R., El-Dorry, H., Faria, J. B., Ferreira, A. J., Ferreira, R. C., Ferro, M. I., Formighieri, E. F., Franco, M. C., Greggio, C. C., Gruber, A., Katsuyama, A. M., Kishi, L. T., Leite, R. P., Lemos, E. G., Lemos, M. V., Locali, E. C., Machado, M. A., Madeira, A. M., Martinez-Rossi, N. M., Martins, E. C., Meidanis, J., Menck, C. F., Miyaki, C. Y., Moon, D. H., Moreira, L. M., Novo, M. T., Okura, V. K., Oliveira, M. C., Oliveira, V. R., Pereira, H. A., Rossi, A., Sena, J. A., Silva, C., de Souza, R. F., Spinola, L. A., Takita, M. A., Tamura, R. E., Teixeira, E. C., Tezza, R. I., Trindade dos Santos, M., Truffi, D., Tsai, S. M., White, F. F., Setubal, J. C., and Kitajima, J. P. (2002) Comparison of the genomes of two *Xanthomonas* pathogens with differing host specificities. *Nature 417*, 459–463.
22. Shi, D., Yu, X., Cabrera-Luque, J., Chen, T. Y., Roth, L., Morizono, H., Allewell, N. M., and Tuchman, M. (2007) A single mutation in the active site swaps the substrate specificity of N-acetyl-L-ornithine transcarbamylase and N-succinyl-L-ornithine transcarbamylase. *Protein Sci. 16*, 1689–1699.
23. Shi, D., Morizono, H., Cabrera-Luque, J., Yu, X., Roth, L., Malamy, M. H., Allewell, N. M., and Tuchman, M. (2006) Structure and catalytic mechanism of a novel N-succinyl-L-ornithine transcarbamylase in arginine biosynthesis of *Bacteroides fragilis*. *J. Biol. Chem. 281*, 20623–20631.
24. Pastra-Landis, S. C., Foote, J., and Kantrowitz, E. R. (1981) An improved colorimetric assay for aspartate and ornithine transcarbamylases. *Anal. Biochem. 118*, 358–363.
25. Shi, D., Yu, X., Roth, L., Morizono, H., Hathout, Y., Allewell, N. M., and Tuchman, M. (2005) Expression, purification, crystallization and preliminary X-ray crystallographic studies of a novel acetylcitrulline deacetylase from *Xanthomonas campestris*. *Acta Crystallogr. F61*, 676–679.
26. Otwinowski, Z., and Minor, W. (1997) Processing of X-ray Diffraction Data Collected in Oscillation Mode. *Methods Enzymol. 276*, 307–326.
27. Collaborative Computational Project, Number 4 (1994) The CCP4 suite: Programs for protein crystallography. *Acta Crystallogr. D50*, 760–763.
28. Jones, T. A., Zou, J. Y., Cowan, S. W., and Kjeldgaard, M. (1991) Improved methods for building protein models in electron density maps and the location of errors in these models. *Acta Crystallogr. A47* (Part 2), 110–119.
29. Brunger, A. T., Adams, P. D., Clore, G. M., DeLano, W. L., Gros, P., Grosse-Kunstleve, R. W., Jiang, J. S., Kuszewski, J., Nilges, M., Pannu, N. S., Read, R. J., Rice, L. M., Simonson, T., and Warren, G. L. (1998) Crystallography & NMR system: A new software suite for macromolecular structure determination. *Acta Crystallogr. D54*, 905–921.
30. Brunger, A. T. (1992) Free R value: A novel statistical quantity for assessing the accuracy of crystal structures. *Nature 355*, 472–475.
31. Laskowski, R. A., MacArthur, M. W., Moss, D. S., and Thornton, J. M. (1993) PROCHECK: A program to check the stereochemical quality of protein structures. *J. Appl. Crystallogr. 26*, 283–291.
32. Golemi, D., Maveyraud, L., Vakulenko, S., Samama, J. P., and Mobashery, S. (2001) Critical involvement of a carbamylated lysine in catalytic function of class D β-lactamases. *Proc. Natl. Acad. Sci. U.S.A. 98*, 14280–14285.
33. Lapko, V. N., Smith, D. L., and Smith, J. B. (2001) In vivo carbamylation and acetylation of water-soluble human lens αB-Crystallin lysine 92. *Protein Sci. 10*, 1130–1136.
34. Shi, D., Morizono, H., Ha, Y., Aoyagi, M., Tuchman, M., and Allewell, N. M. (1998) 1.85-Å resolution crystal structure of human ornithine transcarbamoylase complexed with N-phosphonacetyl-L-ornithine. Catalytic mechanism and correlation with inherited deficiency. *J. Biol. Chem. 273*, 34247–34254.
35. Langley, D. B., Templeton, M. D., Fields, B. A., Mitchell, R. E., and Collyer, C. A. (2000) Mechanism of inactivation of ornithine transcarbamoylase by N^{δ}-(N′-sulfodiaminophosphinyl)-L-ornithine, a true transition state analogue? Crystal structure and implications for catalytic mechanism. *J. Biol. Chem. 275*, 20012–20019.
36. Cha, J., Vakulenko, S. B., and Mobashery, S. (2007) Characterization of the β-lactam antibiotic sensor domain of the MecR1 signal sensor/transducer protein from methicillin-resistant *Staphylococcus aureus*. *Biochemistry 46*, 7822–7831.
37. O'Leary, M. H., Jaworski, R. J., and Hartman, F. C. (1979) ^{13}C nuclear magnetic resonance study of the CO_2 activation of ribulosebisphosphate carboxylase from *Rhodospirillum rubrum*. *Proc. Natl. Acad. Sci. U.S.A. 76*, 673–675.
38. Golemi-Kotra, D., Cha, J. Y., Meroueh, S. O., Vakulenko, S. B., and Mobashery, S. (2003) Resistance to β-lactam antibiotics and its mediation by the sensor domain of the transmembrane BlaR signaling pathway in *Staphylococcus aureus*. *J. Biol. Chem. 278*, 18419–18425.
39. Schneider, K. D., Bethel, C. R., Distler, A. M., Hujer, A. M., Bonomo, R. A., and Leonard, D. A. (2009) Mutation of the active site carboxylysine (K70) of OXA-1 β-lactamase results in a deacylation-deficient enzyme. *Biochemistry 48*, 6136–6145.
40. Huang, C. Y., Hsu, C. C., Chen, M. C., and Yang, Y. S. (2009) Effect of metal binding and posttranslational lysine carboxylation on the activity of recombinant hydantoinase. *J. Biol. Inorg. Chem. 14*, 111–121.
41. Zhang, Q., and Wang, Y. (2008) High mobility group proteins and their post-translational modifications. *Biochim. Biophys. Acta 1784*, 1159–1166.
42. Jabri, E., Carr, M. B., Hausinger, R. P., and Karplus, P. A. (1995) The crystal structure of urease from *Klebsiella aerogenes*. *Science 268*, 998–1004.
43. Young, P. G., Smith, C. A., Metcalf, P., and Baker, E. N. (2008) Structures of *Mycobacterium tuberculosis* folylpolyglutamate synthase complexed with ADP and AMPPCP. *Acta Crystallogr. D64*, 745–753.
44. Gordon, E., Flouret, B., Chantalat, L., van Heijenoort, J., Mengin-Lecreulx, D., and Dideberg, O. (2001) Crystal structure of UDP-N-acetylmuramoyl-L-alanyl-D-glutamate: meso-Diaminopimelate ligase from *Escherichia coli*. *J. Biol. Chem. 276*, 10999–11006.
45. Taylor, T. C., and Andersson, I. (1997) Structure of a product complex of spinach ribulose-1,5-bisphosphate carboxylase/oxygenase. *Biochemistry 36*, 4041–4046.
46. Jensen, R. (2004) Activation of Rubisco controls CO_2 assimilation in light: A perspective on its discovery. *Photosynth. Res. 82*, 187–193.
47. Falkowski, P. G. (1997) Photosynthesis: The paradox of carbon dioxide efflux. *Curr. Biol. 7*, R637–R639.
48. Roos, A., and Boron, W. F. (1981) Intracellular pH. *Physiol. Rev. 61*, 296–434.
49. Smith, K. S., and Ferry, J. G. (2000) Prokaryotic carbonic anhydrases. *FEMS Microbiol. Rev. 24*, 335–366.
50. Bahn, Y. S., and Muhlschlegel, F. A. (2006) CO_2 sensing in fungi and beyond. *Curr. Opin. Microbiol. 9*, 572–578.
51. Esposito, G., Jaiswal, B. S., Xie, F., Krajnc-Franken, M. A., Robben, T. J., Strik, A. M., Kuil, C., Philipsen, R. L., van Duin, M., Conti, M., and Gossen, J. A. (2004) Mice deficient for soluble adenylyl cyclase are infertile because of a severe sperm-motility defect. *Proc. Natl. Acad. Sci. U.S.A. 101*, 2993–2998.
52. Townsend, P. D., Holliday, P. M., Fenyk, S., Hess, K. C., Gray, M. A., Hodgson, D. R., and Cann, M. J. (2009) Stimulation of mammalian G-protein-responsive adenylyl cyclases by carbon dioxide. *J. Biol. Chem. 284*, 784–791.
53. Kwon, J. Y., Dahanukar, A., Weiss, L. A., and Carlson, J. R. (2007) The molecular basis of CO_2 reception in *Drosophila*. *Proc. Natl. Acad. Sci. U.S.A. 104*, 3574–3578.
54. Jones, W. D., Cayirlioglu, P., Kadow, I. G., and Vosshall, L. B. (2007) Two chemosensory receptors together mediate carbon dioxide detection in *Drosophila*. *Nature 445*, 86–90.
55. Xu, Z., Liu, Y., Yang, Y., Jiang, W., Arnold, E., and Ding, J. (2003) Crystal structure of D-Hydantoinase from *Burkholderia pickettii* at a resolution of 2.7 angstroms: Insights into the molecular basis of enzyme thermostability. *J. Bacteriol. 185*, 4038–4049.
56. Sun, T., Nukaga, M., Mayama, K., Braswell, E. H., and Knox, J. R. (2003) Comparison of β-lactamases of classes A and D: 1.5-Å crystallographic structure of the class D OXA-1 oxacillinase. *Protein Sci. 12*, 82–91.
57. Maveyraud, L., Golemi, D., Kotra, L. P., Tranier, S., Vakulenko, S., Mobashery, S., and Samama, J. P. (2000) Insights into class D β-lactamases are revealed by the crystal structure of the OXA10 enzyme from *Pseudomonas aeruginosa*. *Structure 8*, 1289–1298.

58. Benning, M. M., Kuo, J. M., Raushel, F. M., and Holden, H. M. (1995) Three-dimensional structure of the binuclear metal center of phosphotriesterase. *Biochemistry 34*, 7973–7978.
59. Thoden, J. B., Phillips, G. N., Jr., Neal, T. M., Raushel, F. M., and Holden, H. M. (2001) Molecular structure of dihydroorotase: A paradigm for catalysis through the use of a binuclear metal center. *Biochemistry 40*, 6989–6997.
60. Abendroth, J., Niefind, K., and Schomburg, D. (2002) X-ray structure of a dihydropyrimidinase from *Thermus* sp. at 1.3 Å resolution. *J. Mol. Biol. 320*, 143–156.
61. Yang, H., Carr, P. D., McLoughlin, S. Y., Liu, J. W., Horne, I., Qiu, X., Jeffries, C. M., Russell, R. J., Oakeshott, J. G., and Ollis, D. L. (2003) Evolution of an organophosphate-degrading enzyme: A comparison of natural and directed evolution. *Protein Eng. 16*, 135–145.
62. Bertrand, J. A., Auger, G., Martin, L., Fanchon, E., Blanot, D., Le Beller, D., van Heijenoort, J., and Dideberg, O. (1999) Determination of the MurD mechanism through crystallographic analysis of enzyme complexes. *J. Mol. Biol. 289*, 579–590.
63. Park, I. S., and Hausinger, R. P. (1995) Requirement of carbon dioxide for in vitro assembly of the urease nickel metallocenter. *Science 267*, 1156–1158.
64. Sulzenbacher, G., Bignon, C., Nishimura, T., Tarling, C. A., Withers, S. G., Henrissat, B., and Bourne, Y. (2004) Crystal structure of *Thermotoga maritima* α-L-fucosidase. Insights into the catalytic mechanism and the molecular basis for fucosidosis. *J. Biol. Chem. 279*, 13119–13128.
65. Eichman, B. F., O'Rourke, E. J., Radicella, J. P., and Ellenberger, T. (2003) Crystal structures of 3-methyladenine DNA glycosylase MagIII and the recognition of alkylated bases. *EMBO J. 22*, 4898–4909.
66. Burman, J. D., Stevenson, C. E., Sawers, R. G., and Lawson, D. M. (2007) The crystal structure of *Escherichia coli* TdcF, a member of the highly conserved YjgF/YER057c/UK114 family. *BMC Struct. Biol. 7*, 30.